ELSEVIER

Journal of Hazardous Materials 41 (1995) 327–340

JOURNAL OF HAZARDOUS MATERIALS

Reducing the formation of carbon oxides in the production of C_2 hydrocarbons from methane

Sang C. Kim[a,*], Larry E. Erickson[a], Eui Y. Yu[b]

[a]*Center for Hazardous Substance Research, Kansas State University, Manhattan, KS 66506, USA*
[b]*Department of Chemical Engineering, Chonnam National University, Kwangju 500-757, South Korea*

Received 24 June 1994; accepted in revised form 15 November 1994

Abstract

Methane is the main component of natural gas and has been connected with global warming. The oxidative coupling of methane has been studied to enhance C_2 hydrocarbon selectivity and to reduce the formation of carbon oxides associated with C_2 hydrocarbon production. Acid sites of supported catalysts play a role in the formation of carbon oxides. The supported Zn oxide catalyst with α-Al_2O_3 shows no acidity in temperature programmed desorption by using NH_3 and exhibits good C_2 hydrocarbon selectivity. The optimum loading of Zn oxide on α-Al_2O_3 is 60 wt%. The specific surface area of the catalyst appears not to influence activity. Using alkali metal salts as promoter in Zn oxide (60 wt%)/α-Al_2O_3 catalyst, the activity performance for C_2 hydrocarbon formation is LiCl > NaCl > KCl: the performance is well correlated with the apparent molal enthalpy of formation of halides. The activity performance for minimizing carbon oxides is LiCl > KCl > NaCl, which is well correlated with the melting points in alkali halides.

1. Introduction

The applications of catalysts to the treatment of environmental pollution include the cleaning of waste gas, waste water and waste material. To meet the current clean technology, it is necessary to develop new catalyst processes without pollution. The global warming was primarily attributed to the gases such as CFCs, CH_4, nitrogen oxides, and CO_2. The release of CO_2 and CO should be monitored because 60% of global warming comes from CO_2 and because of the toxicity of CO. The effect of methane on global warming is almost twenty times larger than that of CO_2, based on a molecular comparison.

Methane is the most abundant component of natural gas, generally containing over 90 mol% of the hydrocarbons fraction; it is mostly used as an energy source. The

* Corresponding author. Tel.: 1-62-520-7058. Fax: 1-62-527-9250.

0304-3894/95/$09.50
SSDI 0304-3894(94)00112-X

Table 1
Heat of reaction at 298 K for the conversion of methane to several products

Reaction	ΔHr° 298 (Kcal/mol)
$CH_4 + (3/2)O_2 \rightarrow CO + 2H_2O$	− 124.1
$CH_4 + 2O_2 \rightarrow CO_2 + 2H_2O$	− 197.1
$CH_4 + (1/2)O_2 \rightarrow (1/2)C_2H_4 + H_2O$	− 33.6
$CH_4 + (1/4)O_2 \rightarrow (1/2)C_2H_6 + (1/2)H_2O$	− 21.0

utilization of methane for feedstock for the production of hydrocarbon chemicals is limited due to its high molecular stability. Its homolytic bond dissociation energy is 104 Kcal/mol, very similar to hydrogen, but the electronic and symmetrical structure of methane is similar to that of an inert gas; therefore, methane is much less reactive than hydrogen. Because the conversion of methane without an oxidizer is endothermic, a temperature above 800 °C is required to obtain the efficient conversion, but the formation of $CO_x(=CO + CO_2)$ is more favorable than the formation of $C_2(=C_2H_4 + C_2H_6)$ under the oxidation conditions; that is, at 298 K, the heat of reaction varies as shown in Table 1.

Since the pioneering work on the oxidative coupling of methane by Keller and Bhasin [1], the conversion of methane to C_2 and larger hydrocarbons has been investigated in several laboratories [2–7].

Generally, the mechanism of oxidative coupling of methane is well known; a methyl radical may be produced on the surface of catalyst; ethane is produced by the coupling of two methyl radicals, and then ethylene is produced by the dehydrogenenation of ethane [8, 9]. The formation of $CO_x(=CO + CO_2)$ can be described, by the following two schemes [10]:

Surface methoxide scheme:

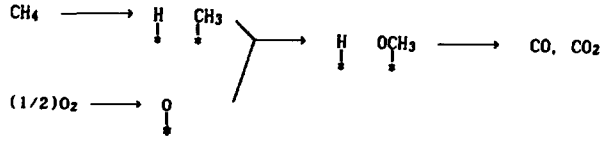

Surface peroxide scheme:

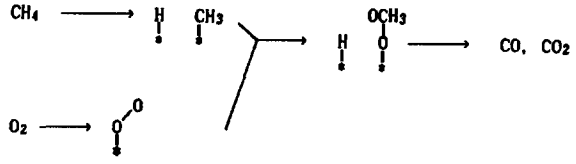

where * represents an active site.

Different kinds of supports have been extensively studied by many research groups [11–14] to enhance the activity of the catalyst, but the data about Zn oxide are very

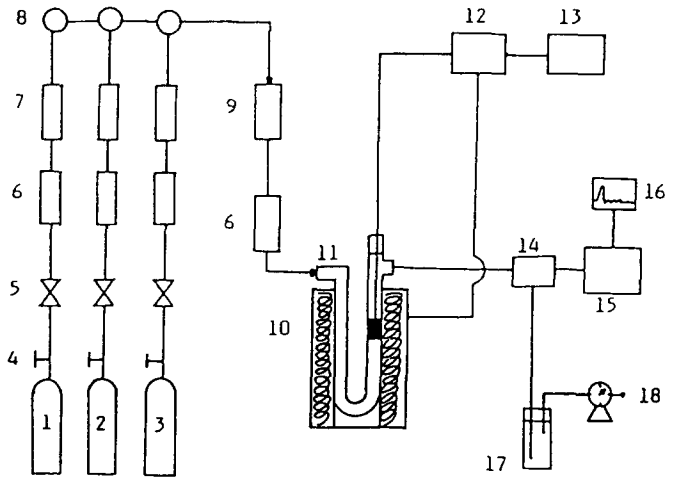

Fig. 1. Schematic diagram of experimental apparatus: (1) N_2 cylinder; (2) O_2 cylinder; (3) CH_4 cylinder; (4) pressure regulator; (5) needle valve; (6) silica trap; (7) capillary flow meter; (8) three way cock; (9) mixing chamber; (10) electric furnace; (11) reactor; (12) temperature recorder; (14) gas sampler; (15) G.C.; (16) data processor; (17) bubble trap; (18) wet gas meter.

limited. The objective of this study is to enhance the C_2 hydrocarbon selectivity and reduce the formation of carbon oxides; Zn oxide has been used as host catalyst. The effects of alkali promoters and the supports have also been investigated.

2. Experimental methods

2.1. Catalyst preparation

$Zn(NO_3)_2 \cdot 6H_2O$, which was commercial, was dissolved in deionized water, and then added to NH_4OH aqueous solution. The product was precipitated in the range of pH 9–10, and then washed and filtered several times by using deionized water until the solution was at pH 7. The resulting material, $Zn(OH)_2$ was dried in an oven at 125 °C for 24 h. A constant amount of $Zn(OH)_2$ and each support (α-Al_2O_3, γ-Al_2O_3, SiO_2), which were 150–200 mesh, respectively, were added into a solution where an alkali promoter (NaCl, KCl or LiCl) was dissolved in deionized water. The resulting slurry was heated by stirring to evaporate excess water until a thick paste remained. The thick paste was then dried in an oven at 125 °C for 14 h and was calcined in air at 800 °C for 6 h; thereafter it was powdered.

2.2. Apparatus

The schematic diagram of the experimental apparatus is shown in Fig. 1; a conventional fixed bed flow reactor in the shape of a U is employed. The dimensions of the

reactor were 1.1 cm ID and 38 cm long for the inlet section and 0.5 cm ID and 29 cm long for the outlet section. The catalyst (0.5 g) was mechanically mixed with sea sand (3 g) as diluent before being packed into the reactor to obtain a nearly uniform dispersion of the catalyst which results in better yields of hydrocarbons and a more uniform temperature distribution. The catalyst was held in place by a small plug of quartz wool. The reactor was heated in a tubular furnace to a desirable temperature and the temperature was controlled within an accuracy of $\pm$ 1.0 °C using a temperature controller. In most experiments, flow rates of methane and oxygen were 4 cc/min and 2 cc/min, respectively. The CH_4/O_2 molar ratio was 2 because this is the stoichiometric ratio for conversion of CH_4 and O_2 to C_2H_4 and H_2O. The total flow rates were maintained at 50 cc/min by adding the balance gas, N_2.

The gaseous reactants were mixed in a mixing chamber which was packed with Raschig rings, and then purified by passing them through purifier that contained blue silica gel and molecular sieve. The effluent gases were analyzed by an on-line gas chromatograph (model 7AG, Shimadzu Co., Japan) system, using the porapak Q column (3 mm, 3 m long, 60–80 mesh, 90 °C) for methane, carbon dioxide, ethylene, ethane and water and the molecular sieve 5A column (3 mm, 3 m long, 60–80 mesh, 90 °C) for oxygen and carbon monoxide.

The characterization of the catalysts was studied by X-ray powder diffraction (XRD, Geigerflex, Rigaku) and a differential thermal analysis (TG-DTA, STA1640, Stanton Redcroft). The BET surface areas were determined by nitrogen physisorption at $-$ 196 °C, using a Micromeritics ASAP2000 system.

The activity of the catalyst was determined with three terms which were defined below.

$$\% \text{ Conversion} = [(\text{moles of converted methane})/(\text{moles of methane input})] \times 100,$$

$$\% \text{ Selectivity} = [(\text{moles of converted methane into the desired component products})/(\text{moles of converted methane})] \times 100,$$

$$\% \text{ Yield} = [(\text{moles of converted methane into the desired products})/(\text{moles of methane input})] \times 100.$$

3. Results and discussion

3.1. *Effect of supports*

Table 2 shows the results which were obtained with the 20 wt% loading of Zn oxide on the various supports: α-Al_2O_3 ($S_{BET} \leqslant 1$ m^2/g), γ-Al_2O_3 ($S_{BET} = 166$ m^2/g) and SiO_2 ($S_{BET} = 208$ m^2/g). The conversion, the C_2 and CO_x selectivities are 11%, 26% and 74%, respectively, using Zn oxide catalyst. The conversion is reduced to 1.8% and also the CO_x selectivity reduced over Zn oxide (20 wt%)/α-Al_2O_3 catalyst. The conversion increases to 19% over Zn oxide (20 wt%)/γ-Al_2O_3, and the CO_x selectivity 100%. The conversion is 6.7% and the CO_x selectivity is 83% over Zn oxide

Table 2
Influence of support on the catalytic activity

Catalyst	Conversion[a] (%)	Selectivity[a] (%)		
		$C_2(=C_2H_4+C_2H_6)$	CO	CO_2
Zn oxide	11	26	3.0	71
Zn oxide 20 wt%)/α-Al_2O_3	1.8	59	16	24
Zn oxide (20 wt%)/γ-Al_2O_3	19	0.0	7.0	93
Zn oxide (20 wt%)/SiO_2	6.7	16	14	69

Reaction conditions: Catalyst 0.5 g, Total flow rate = 50 cc/min; methane flow rate = 4 cc/min; oxygen flow rate = 2 cc/min; reaction temp. = 750 °C.
[a] The error ranges from ±0.05% to ±4%.

Table 3
Influence of NaCl on the catalytic activity

Catalyst	Conversion[a] (%)	Selectivity[a] (%)		
		$C_2(=C_2H_4+C_2H_6)$	CO	CO_2
NaCl (20 wt%)/Zn oxide (20 wt%)/α-Al_2O_3	9.3	61	24	16
NaCl (20 wt%)/Zn oxide (20 wt%)/γ-Al_2O_3	19	19	17	64
NaCl (20 wt%)/Zn oxide (20 wt%)/SiO_2	7.2	57	19	24

Reaction conditions: Catalyst = 0.5 g, Total flow rate 50 cc/min; methane flow rate = 4 cc/min; oxygen flow rate = 2 cc/min; reaction temp. = 750 °C.
[a] The error ranges from ± 0.05 % to ± 14 %.

(20 wt%)/SiO_2. When γ-Al_2O_3 and SiO_2 in Zn oxide catalyst are used as supports, the formation of CO_x is favored. The above results indicate that the specific surface area may not play a dominant role in the formation of CO_x, since the specific surface area of SiO_2 is larger than that of γ-Al_2O_3. It is well known that the acid sites on the catalyst can produe CO_x from hydrocarbons [15].

It is shown in Table 3 that better results are obtained using the 20 wt% NaCl added to each catalyst. Where Zn oxide catalysts were supported with γ-Al_2O_3 and SiO_2, promoted with NaCl, the conversion is similar to the catalyst without NaCl; the CO_x selectivity is considerably reduced, but the C_2 selectivity is enhanced. It is supposed that alkali metal salt may neutralize the acid sites on Zn oxide (20 wt%)/γ-Al_2O_3 and Zn oxide (20 wt%)/SiO_2, which will increase the C_2 selectivity. To confirm the correlation between the acid sites and the C_2 selectivity, a temperature programmed desorption (TPD) of ammonia was carried out. The result is shown in Fig. 2. The magnitude of the acid sites in each catalyst is directly related to the CO_x selectivity. For example, Zn oxide (20 wt%)/α-Al_2O_3 and NaCl (20 wt%)/Zn oxide (20 wt%)/α-Al_2O_3, which show the smallest CO_x selectivity did not desorb very much ammonia in

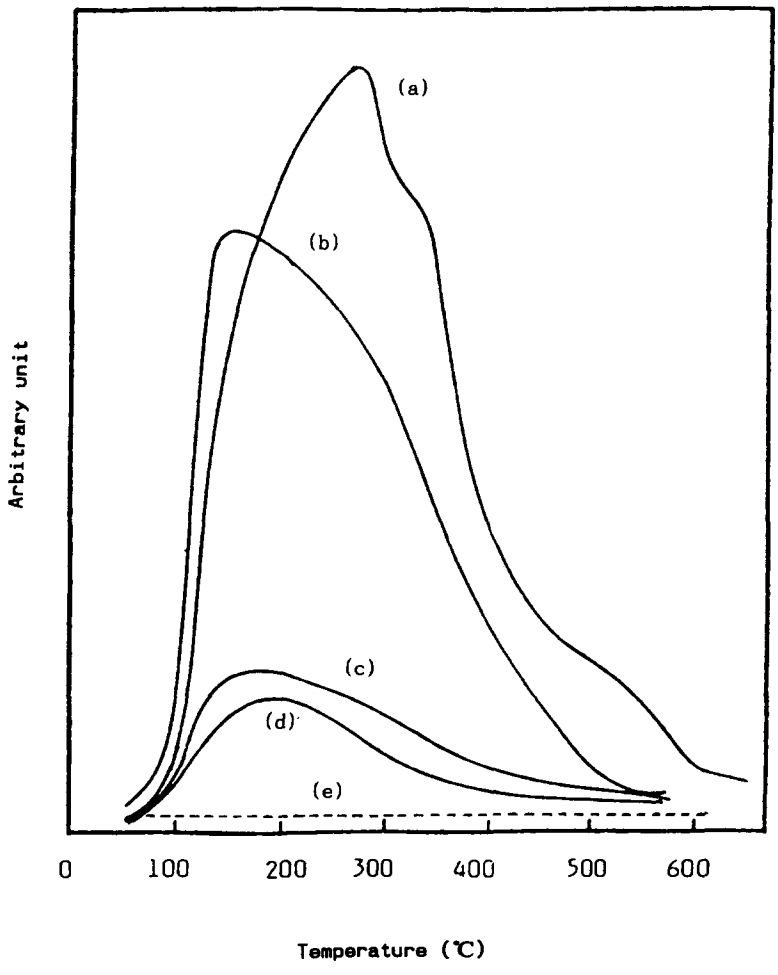

Fig. 2. TPD graph of ammonia desorption for various catalysts: (a) Zn oxide (20 wt%)/γ-Al_2O_3; (b) NaCl (20 wt%)/Zn oxide (20 wt%)/γ-Al_2O_3; (c) Zn oxide (20 wt%)/SiO_2; (d) NaCl (20 wt%)/Zn oxide (20 wt%)/γ-SiO_2; (e) Zn oxide (20 wt%)/α-Al_2O_3; NaCl (20 wt%)/Zn oxide (20 wt%)/α-Al_2O_3.

the TPD experiment. Therefore, it is concluded that the acid sites on the catalyst play an important role in the formation of CO_x from methane.

Table 4 reveals the activities for catalysts with different contents of Zn oxide, supported with α-Al_2O_3, at 750 °C. The conversion increases with increasing Zn oxide content and becomes constant after 40 wt%. The C_2 selectivity decreases with increasing the Zn oxide content, but increase at 50 wt%, shows a local maximum at 60 wt%, and then decreases again above the 60 wt%. For the C_2 and the CO_x yield, Zn oxide (60 wt%)/α-Al_2O_3 is shown as the optimum Zn oxide content. For this type of local maximum in the C_2 selectivity, "Isolated Site" type reaction, which was suggested by Agarwal et al. [16], can be considered.

Table 4
Influence of zinc concentration on the catalytic activity

Catalyst	Conversion[a] (%)	Selectivity[a] (%)		
		$C_2(=C_2H_4 + C_2H_6)$	CO	CO_2
Zn oxide (20 wt%)/α-Al_2O_3	1.8	59	16	24
Zn oxide (30 wt%)/α-Al_2O_3	3.0	60	13	27
Zn oxide (40 wt%)/α-Al_2O_3	11	33	7.9	59
Zn oxide (50 wt%)/α-Al_2O_3	10	43	6.4	51
Zn oxide (60 wt%)/α-Al_2O_3	11	51	7.2	42
Zn oxide (70 wt%)/α-Al_2O_3	11	43	6.7	50

Reaction conditions: Catalyst = 0.5 g, Total flow rate = 50 cc/min; methane flow rate = 4 cc/min; oxygen flow rate = 2 cc/min; reaction temp. = 750 °C.
[a] The error ranges from ± 0.05% to ± 4%.

Fig. 3 shows the result when the catalysts in Table 4 were analyzed by using XRD. With the change of Zn oxide from 20 wt% to 70 wt% in Zn oxide/α-Al_2O_3 catalyst, only the ZnO and α-Al_2O_3 crystal phase exist. The results of XRD analysis support "Isolated Site" type reaction.

3.2. *Effect of alkali metal salt promoter*

In the previous section, Zn oxide (60 wt%)/α-Al_2O_3 catalyst appeared as the optimum catalyst. Fig. 4 shows the conversion and selectivity for the different NaCl contents added to Zn oxide (60 wt%)/α-Al_2O_3 at 750 °C. Increasing the NaCl content increases the conversion. The C_2 selectivity is a maximum and the CO_x selectivity the minimum at 5 wt% NaCl content. The C_2 selectivity decrease above 5 wt% NaCl content.

Fig. 5 shows the results when the catalysts in Fig. 4 were analyzed by using XRD. No NaCl peak appears at 5 wt% NaCl content but the NaCl peak appears for 10 wt% NaCl content and higher contents. Since NaCl is uniformly distributed on Zn oxide (60 wt%)/α-Al_2O_3 at 5 wt% NaCl content, NaCl crystal phase may not appear [17]. It is well known that Cl radical catalyzes the formation of ethylene from methane in the gas phase [18].

$$CH_4 + Cl\cdot \rightarrow CH_3\cdot + HCl$$

$$2CH_3\cdot \rightarrow C_2H_6$$

$$C_2H_6 + Cl\cdot \rightarrow HCl + C_2H_5\cdot$$

$$C_2H_5\cdot \rightarrow H\cdot + C_2H_4$$

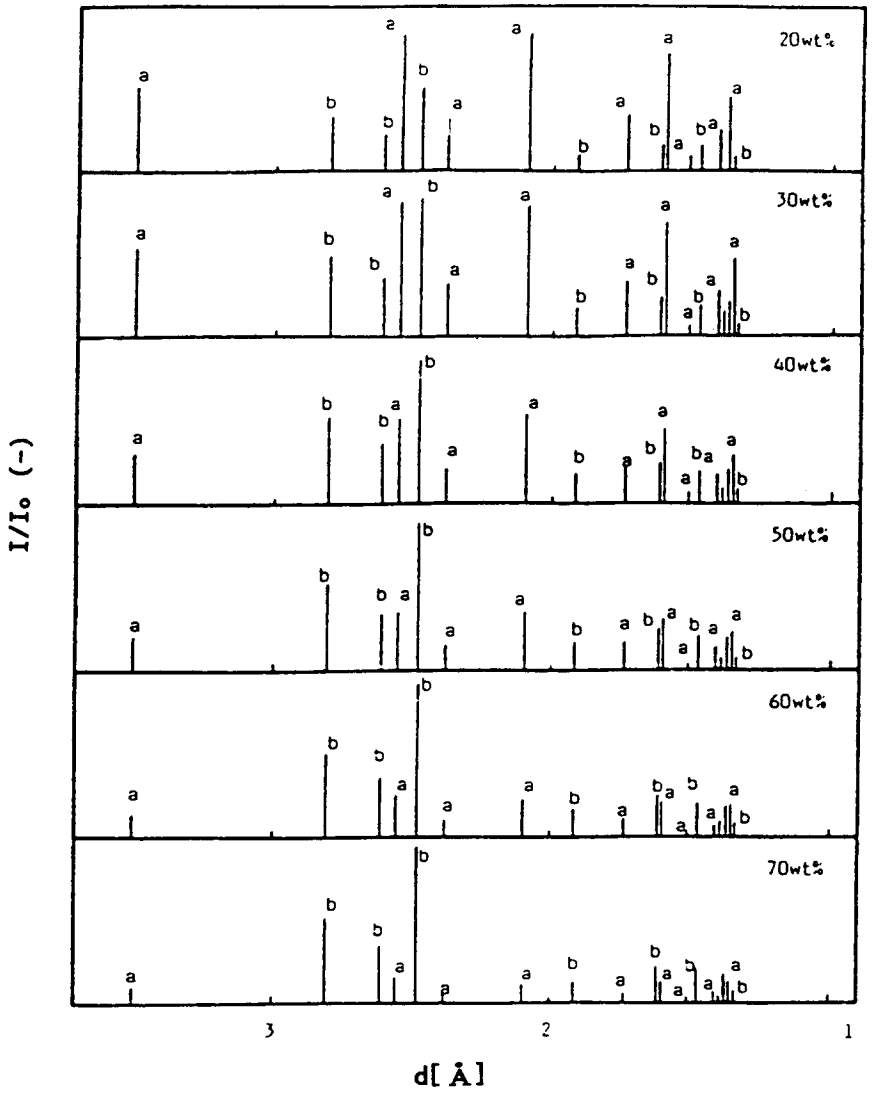

Fig. 3. XRD patterns of Zn oxide catalysts supported with α-Al_2O_3. a: α-Al_2O_3; b: ZnO.

When NaCl which contains Cl is used as promoter, the beneficial effect can be obtained according to following mechanism [19]:

$$NaCl + CH_4 + (\tfrac{1}{2})O_2 \rightarrow NaOH + CH_3Cl\cdot.$$

Our preceding paper [20] reported that the affinity between Na^+ and Cl^- might be weakened on the metal oxide. Therefore, as shown in Fig. 4, it can be used to explain

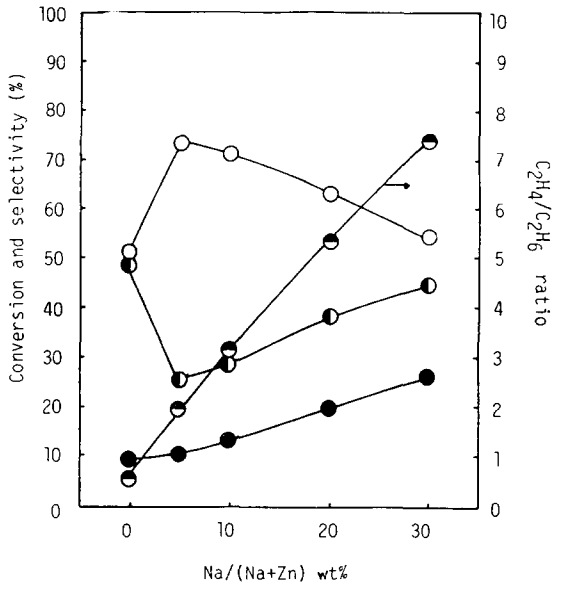

Fig. 4. Effect of NaCl content in Zn oxide (60 wt%)/α-Al_2O_3 catalyst: Reaction temperature = 750 °C; conversion: CH_4 (●); selectivity: C_2 (○), CO_x (◐); C_2H_4/C_2H_6 ratio (◓).

that increasing the NaCl content increases the formation ratio of ethylene/ethane from the above mechanism. It is also well known that CO and CO_2 may be produced via methoxide or methyl peroxy radical [8, 21]. As shown in Fig. 4, increasing the NaCl content increases the CO_x selectivity. The formation rate of ethane which is made from coupling with two methyl radicals, is proportional to (methyl radical)$^{1/2}$ and the formation rates ($CH_3\cdot + O_2 \rightarrow CH_3O_2\cdot$, $CH_3\cdot + (\frac{1}{2})O_2 \rightarrow CH_3O\cdot$) is proportional to (methyl radical)^1, therefore, increasing the formation rate of methyl radical also is favorable to the latter. In considering the above suggested mechanism, increasing the NaCl content increases both the conversion and the CO_x selectivity. Also, the results of Table 5 support well the role of Cl in the oxidative coupling of methane.

In the preceding paper [19], it was reported that the melting points of alkali halide promoters were correlated with the C_2 yield. The melting points of LiCl, KCl and NaCl are 610 °C, 711 °C an 801 °C [22], respectively. In Table 5, the best results were obtained with LiCl as the promoter.

Differential thermal analysis (DTA) results for the above three catalysts are shown in Fig. 6. The peaks shown below 200 °C are endothermic peaks of water and the endothermic peaks shown above 200 °C correspond to the melting points of each promoter. As shown in Table 5, the activity order is LiCl > NaCl > KCl in the Zn oxide (60 wt%)/α-Al_2O_3 catalyst system at 750 °C.

Fig. 7 shows the effect of the apparent molal enthalpy of formation in alkali halides on the C_2 yield. The larger is the absolute value of the apparent molal enthalpy of

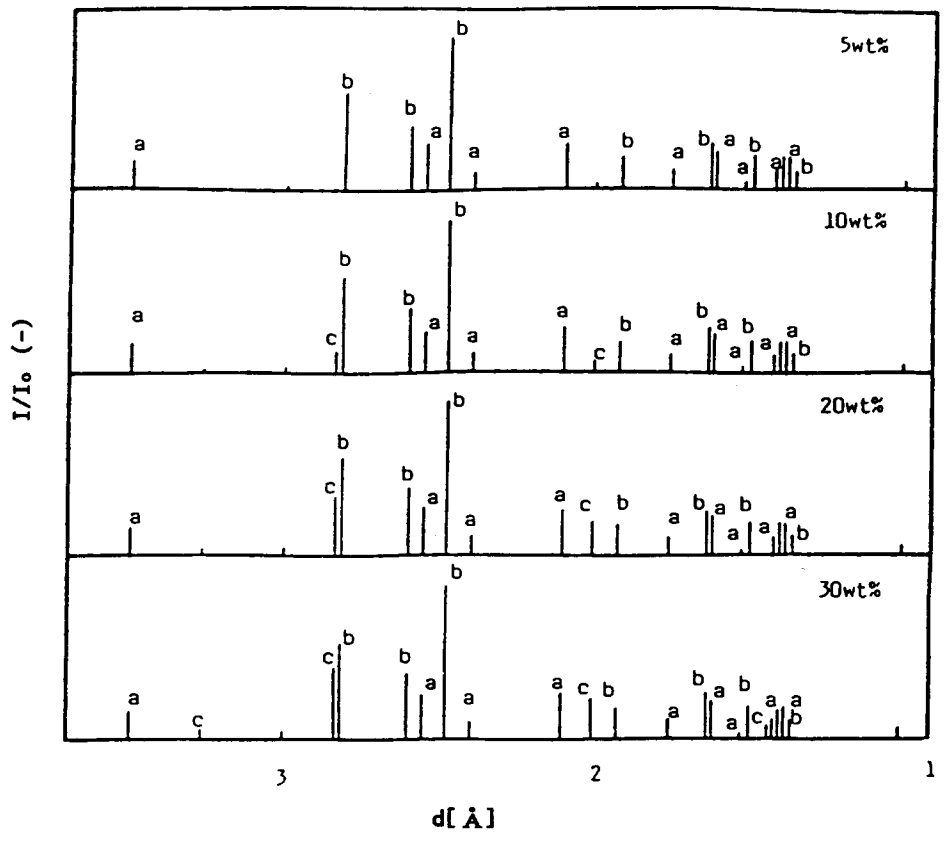

Fig. 5. XRD patterns of various NaCl contents in Zn oxide (60 wt%)/α-Al_2O_3 catalyst: (a) α-Al_2O_3, (b) ZnO, (c) NaCl.

Table 5
Influence of alkali metal chloride on the catalytic activity

Catalyst	Conversion[a] (%)	Selectivity[a] (%)			
		C_2H_4	C_2H_6	CO	CO_2
Zn oxide (60 wt%)/α-Al_2O_3 NaCl (30 wt%)/	11	18	33	7.2	16
Zn oxide (60 wt%)/α-Al_2O_3 LiCl (30 wt%)/	27	49	6.4	32	13
Zn oxide (40 wt%)/α-Al_2O_3 KCl (30 wt%)/	29	78	1.8	14	6.9
Zn oxide (50 wt%)/α-Al_2O_3	16	51	17	5.2	27

Reaction conditions: Catalyst = 0.5 g, Total flow rate = 50 cc/min; methane flow rate = 4 cc/min; oxygen flow rate = 2 cc/min; reaction temp. = 750 °C.

[a] The error ranges from ± 0.05% to ± 4%.

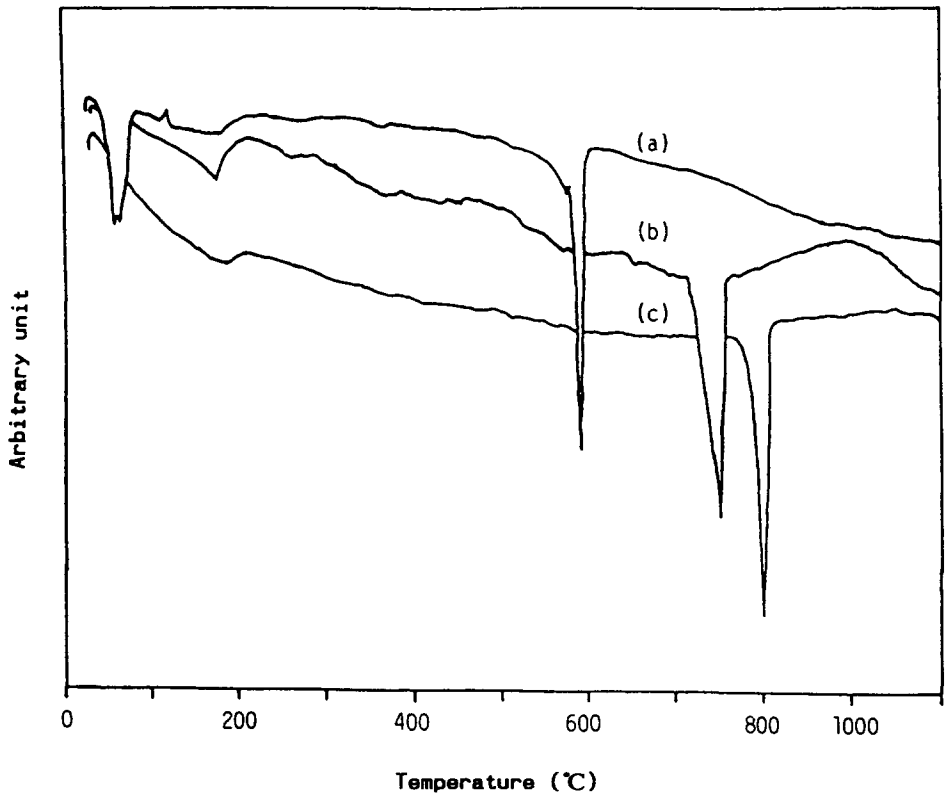

Fig. 6. DTA graph of various catalysts: (a) LiCl (30 wt%)/Zn oxide (60 wt%)/α-Al_2O_3; KCl (30 wt%)/Zn oxide (60 wt%)/α-Al_2O_3; (c) NaCl (30 wt%)/Zn oxide (60 wt%)/α-Al_2O_3.

formation in alkali halides, the more difficult it is to dissociate alkali halides; subsequently, it is difficult to release Cl in alkali halides. In considering between the apparent molal enthalpy of formation in alkali halides and the C_2 yield, the activity order should be LiCl > NaCl > KCl. It is shown in Fig. 7 that the C_2 yield decreases as the magnitude of the apparent molal enthalpy of formation of alkali halides increases. From the standpoint of reducing the formation of CO_x, the activity order is LiCl > KCl > NaCl in the Zn oxide (60 wt%)/α-Al_2O_3 catalyst system. LiCl and KCl in Zn oxide (60 wt%)/α-Al_2O_3 could be melted at 750 °C. The result indicates that alkali metal halides, when melted, may poison the active site for CO_x in the catalysts [23].

3.3. *Effect of the reaction temperature*

Fig. 8 shows the effect of reaction temperature on the formation rate of each product and the C_2 selectivity over NaCl (30 wt%)/ZnO (60 wt%)/α-Al_2O_3. With

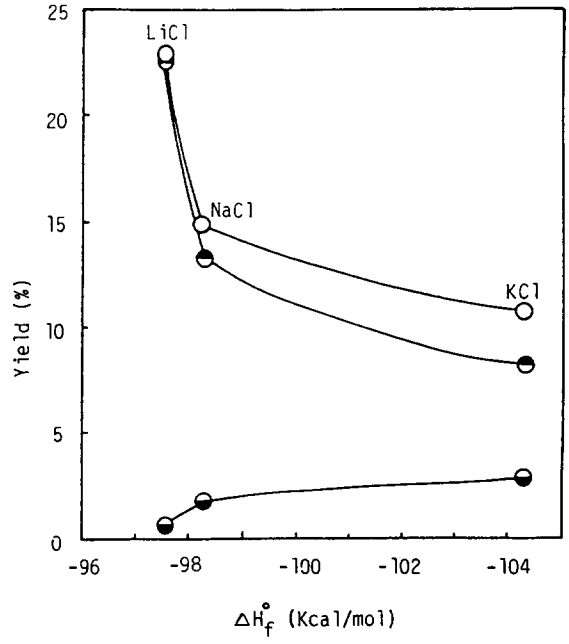

Fig. 7. Effect of the apparent molal enthalpy of formation in alkali halides over Zn oxide (60 wt%)/α-Al_2O_3 catalyst: Reaction temperature = 750 °C; yield: C_2 (○), C_2H_4 (◓), C_2H_6 (◒).

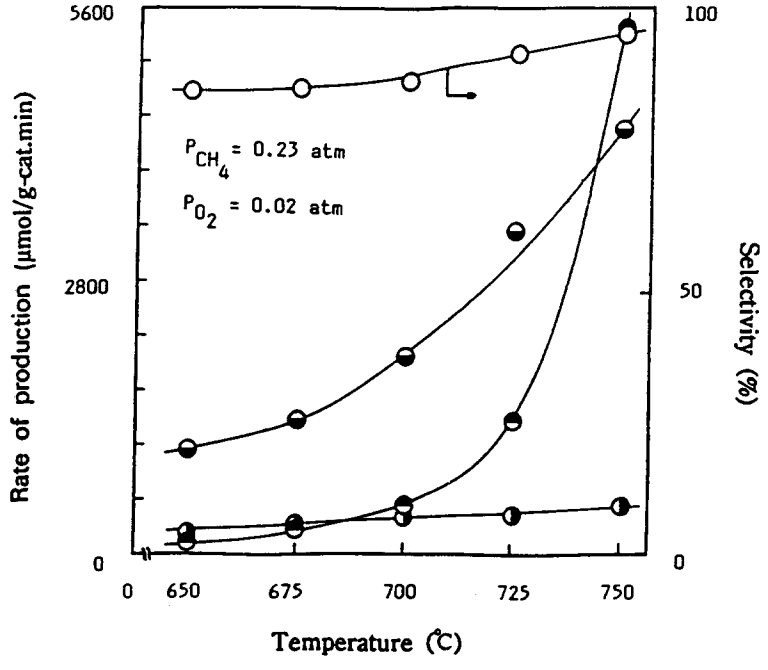

Fig. 8. Effect of reaction temperature on the rates of formation of products and on the C_2 selectivity over NaCl (30 wt%)/Zn oxide (60 wt%)/α-Al_2O_3 catalyst: P_{CH_4} = 0.23 atm, P_{O_2} = 0.02 atm; total flow rate = 100 cc/min; the rate of formation of the products: C_2H_4 (◓), C_2H_6 (◒), CO_x (◑); selectivity: C_2 (○).

increasing reaction temperature, the formation rate of CO_x slowly increases, that of ethane increases rapidly. The formation rate of ethylene increases below 700 °C and rapidly above 725 °C. The C_2 selectivity also increases with increasing reaction temperature. It is observed that raising the reaction temperature under the reaction condition is favorable to the order of $C_2H_4 > C_2H_6 > CO_x$. This result is corresponding to the thermodynamic theory in Table 1.

4. Conclusions

1. The acid sites of supported catalysts have enhanced the CO_x selectivity. α-Al_2O_3 which does not exhibit acid sites has been chosen as a good support. The optimum loading of Zn oxide on α-Al_2O_3 is 60 wt%. The specific surface area of the catalyst does not appear to be associated with the activity.

2. When alkali halides are added as promoters to Zn oxide (60 wt%)/α-Al_2O_3, the activity order of catalyst is LiCl > NaCl > KCl, and the activity order is correlated with the apparent molal enthalpy of the promoter. When reducing the formation of CO_x is considered, the activity order is LiCl > KCl > NaCl and the activity order is correlated with the melting point of each promoter. The best results were obtained with LiCl as promoter.

References

[1] G.E. Keller and M.M. Bhasin, Synthesis of ethylene via oxidation coupling of methane, J. Catal., 73 (1982) 9.
[2] M.O. Lo, S.K. Agrawal and G. Marcelin, Oxidative coupling of methane over antimoney-based catalysts, J. Catal., 112 (1988) 168.
[3] S. Wada, T. Tagawa and H. Imai, Kinetics and mechanism of oxidative coupling of methane over lanthanum–boron oxide, Appl. Catal., 47 (1989) 277.
[4] Y. Osada, S. Koike, T. Fukushima and S. Ogasawara, Oxidative coupling of methane over Y_2O_3–CaO catalysts, Appl. Catal., 59 (1990) 59.
[5] J.M. Aigler and J.H. Lunsford, Oxidative dimerization of methane over MgO and Li^+MgO monoliths, Appl. Catal., 70 (1991) 29.
[6] L. Lehmann and M. Baerns, Kinetic studies of the oxidative coupling of methane over NaOH/CaO catalyst, J. Catal., 135 (1992) 467.
[7] Y. Jiang, I.V. Yentekakis and C.G. Vayenas, Methane to ethylene with 85 percent yield in a gas recycle electrocatalytic reactor–separator, Science, 264 (1994) 1563.
[8] J.A. Sofranko, J.J. Leonard and C.A. Jones, The oxidative coupling of methane to higher hydrocarbons, J. Catal., 103 (1987) 302.
[9] Y. Ohtsuka, M. Kuwabara and A. Tomita, Selective oxidative coupling of methane to ethylene with molten oxides containing alkali metal chloride, Appl. Catal., 47 (1989) 307.
[10] R. Pitchai and K. Klier, Partial oxidation of methane, Catal. Rev. Sci. Eng., 28(1) (1986) 13.
[11] K. Otsuka and T. Komatsu, Conversion of methane to aromatic hydrocarbons by combination of catalysts, Chem. Lett., (1986) 1955.
[12] D.J. Driscoll, W. Martir, J.X. Wang and J.H. Lunsford, Formation of gas-phase methyl radicals over MgO, J. Am. Chem. Soc., 107 (1985) 58.
[13] H.S. Zhang, J.X. Wang, D.J. Driscoll and J.H. Lunsford, Activation and oxidative dimerization of methane over lithium-promoted zinc oxide, J. Catal., 112 (1988) 366.

[14] C.A. Jones, J.J. Leonard and J.A. Sofranko, The oxidative conversion of methane to higher hydrocarbons over alkali-promoted Mn/SiO_2, J. Catal., 103 (1987) 311.
[15] K. Otsuka, M. Hatano and T. Komatsu, in D.M. Bibby et al. (Eds.), Methane Conversion, Elsevier, Amsterdam, 1988, p. 383.
[16] S.K. Agarwal, R.A. Migone and G.M. Marcelin, Oxidative Coupling of Methane, Elsevier, Amsterdam, 1988, p. 383.
[17] C.H. Satterfield, Heterogeneous Catalysis in Practice, 1st edn., McGraw-Hill, New York, 1980, 126.
[18] M. Weissman and S.W. Benson, Pyrolysis of methyl chloride, a pathway in the chlorine-catalyzed polymerization of methane, Int. J. Chem. Kinet., 16 (1984) 307.
[19] S.C. Kim and E.Y. Yu, The oxidative coupling of methane over supported zinc oxide catalyst with alkali promoters, HWAHAK KONGHAK, 28(5) (1990) 536.
[20] S.C. Kim, C.S. Sunwoo and E.Y. Yu, The effect of alkali promoters in oxidative coupling of methane with Mn-oxide catalysts, Korean J. Chem. Eng., 7(4) (1990) 279.
[21] T. Ito, J.X. Wang, C.H. Lin and J.H. Lunsford, Oxidative dimerization of methane over a lithium-promoted magnesium oxide catalyst, J. Am. Chem. Soc., 107 (1985) 5062.
[22] J.A. Dean, Langes's Handbook of Chemistry, 12th edn., McGraw-Hill, New York, 1979.
[23] K. Otsuka, M. Hatano and T. Komatsu, in: Proc. 1st Workshop Catalytic Methane Conversion. Bochum, 1988, Catal. Today, 4 (1989) 409.